

Forced translocation of a polymer: dynamical scaling vs. MD-simulation

J. L. A. Dubbeldam², V. G. Rostiashvili¹, A. Milchev^{1,3}, and T.A. Vilgis¹

¹ *Max Planck Institute for Polymer Research, 10 Ackermannweg, 55128 Mainz, Germany*

² *Delft University of Technology 2628CD Delft, The Netherlands*

³ *Institute for Physical Chemistry, Bulgarian Academy of Sciences, 1113 Sofia, Bulgaria*

We suggest a theoretical description of the force-induced translocation dynamics of a polymer chain through a nanopore. Our consideration is based on the tensile (Pincus) blob picture of a pulled chain and the notion of propagating front of tensile force along the chain backbone, suggested recently by T. Sakaue. The driving force is associated with a chemical potential gradient that acts on each chain segment inside the pore. Depending on its strength, different regimes of polymer motion (named after the typical chain conformation, “trumpet”, “stem-trumpet”, etc.) occur. Assuming that the local driving and drag forces are equal (i.e., in a quasi-static approximation), we derive an equation of motion for the tensile front position $X(t)$. We show that the scaling law for the average translocation time $\langle\tau\rangle$ changes from $\langle\tau\rangle \sim N^{2\nu}/f^{1/\nu}$ to $\langle\tau\rangle \sim N^{1+\nu}/f$ (for the free-draining case) as the dimensionless force $\tilde{f}_R = aN^\nu f/T$ (where a , N , ν , f , T are the Kuhn segment length, the chain length, the Flory exponent, the driving force, and the temperature, respectively) increases. These and other predictions are tested by Molecular Dynamics (MD) simulation. Data from our computer experiment indicates indeed that the translocation scaling exponent α grows with the pulling force \tilde{f}_R albeit the observed exponent α stays systematically smaller than the theoretically predicted value. This might be associated with fluctuations which are neglected in the quasi-static approximation.

PACS numbers: 82.37.-j, 82.35.Lr, 87.15.A-

I. INTRODUCTION

The force-induced translocation through a pore in the membrane is mainly motivated by the possibility for fast DNA and RNA sequencing [1, 2]. Translocation dynamics is an essential component of transport in biological cells [3]. Most of the experimental studies so far deal with a driven polymer translocation which is realized by applying an electrical field across a narrow pore [4]. However, despite extensive research, numerous computer experiments, and a variety of attempts for theoretical interpretations, the translocation dynamics even in the generic case remains at present insufficiently well understood [5–12]. As emphasized in a recent review paper [13], currently there exists a plethora of theoretical predictions for the value of the translocation exponent α which governs the scaling of the mean translocation time $\langle\tau\rangle$ with the length N of the polymer chain ($\langle\tau\rangle \propto N^\alpha$). These values vary in a rather broad interval: one predicts $\alpha = 1$ [5, 6, 8], or $\alpha = 2\nu + 1 - \gamma_1 \approx 1.49$ [10] for a three-dimensional (3D) self-avoiding (SAW) polymer chain (where the Flory exponent $\nu \approx 0.59$ and the surface exponent $\gamma_1 \approx 0.68$), up to $\alpha = (1 + 2\nu)/(1 + \nu) \approx 1.37$ [11] and $\alpha = 1 + \nu \approx 1.59$ [9, 12].

In a recent paper [14] we demonstrated that the dynamics of a single polymer moving through a nanopore in a membrane (i.e. the translocation dynamics) with or without an external force being present can be treated within the framework of fractional Brownian motion (fBm). It was shown that the corresponding Fokker-Planck equation of motion (FPEM) contains time-dependent drift and diffusion terms. In the case of non-driven chain this FPEM leads naturally to anomalous diffusion of the translocation coordinate $s(t)$ [14] that describes the number of segments threaded through the pore at time t . On the other hand, for a driven translocation fluctuations play a relatively moderate role and one can directly construct reasonable scaling relations that describe the process. Recently, an interesting approach based on the notion of tensile force propagation along the chain (within the well known picture of tensile blobs [20, 21]) has been suggested by T. Sakaue [15, 16] in an effort to provide a consistent description of translocation dynamics. Sakaue’s approach appears physically sound and well capable of providing a plausible interpretation of existing observation. However, his mathematical treatment requires the use of a “cut-off” trick as applied to the polymer segments density function (see more details in the Appendix A). This trick is questionable and affects the predicted translocation exponent α .

In the present paper we follow Sakaue’s approach and consider theoretically the case of a driven translocation by means of a different derivation which does not require additional conjectures. In Sec. II we investigate the various regimes (named traditionally a “trumpet”, “stem-trumpet”, and “stem” regimes), observed for weak, intermediate and strong driving forces. Our consideration is based on equating the driving and drag forces, i.e., on a *quasi-static approximation* whereby fluctuations in this balance of forces are ignored. Our main concern is the scaling law for the mean translocation time $\langle\tau\rangle$ with respect to the chain length N and the applied driving force f . We find $\langle\tau\rangle \propto N^\alpha f^{-\delta}$ albeit with a different expression for α as well as the mean translocated length $M(t)$ vs. time.

We also perform extensive Molecular Dynamics (MD) simulations in order to test our theoretical predictions. In Sec. III we describe the simulation model and compare theoretical predictions with simulation data. This comparison shows that the exponent α , found in MD-simulation, is systematically smaller than its theoretical estimate even though α changes with f as expected. We argue that this may be due to fluctuations which are neglected in the theoretical treatment. Finally, in the Appendix A we explain in detail why the calculations of Sakaue [15, 16] are bound to produce a scaling exponent that differs from the proper one.

II. DYNAMICAL SCALING PICTURE OF A DRIVEN TRANSLOCATION

A. A general overview

We assume that the pulling force is applied only to a bead which is inside the pore, i.e., the potential drops mainly across the pore. This assumption was recently examined for charged DNA translocations [17, 18]. It was shown, in particular, that the ionic current generates a nonuniform electric field which is extended far beyond the pore and acts on both the DNA and its counter ions. In this case the DNA threading through the pore is preceded by its capture by electroosmotic flow. On the other hand, it can be shown that for a sufficiently narrow pore the voltage drop mainly takes place inside the pore [19]. In this situation the translocation is mainly determined by the threading process which is the main subject of our investigation.

When a pulling force is suddenly switched on, tension starts to propagate along the chain backbone which alters the polymer conformation progressively. Eventually, after some characteristic time a steady state is reached and the whole polymer starts moving with constant velocity. Such a non-equilibrium response is of great importance in many biological and technological situations. Below we follow to some extent the model developed in the recent papers by Sakaue [15, 16].

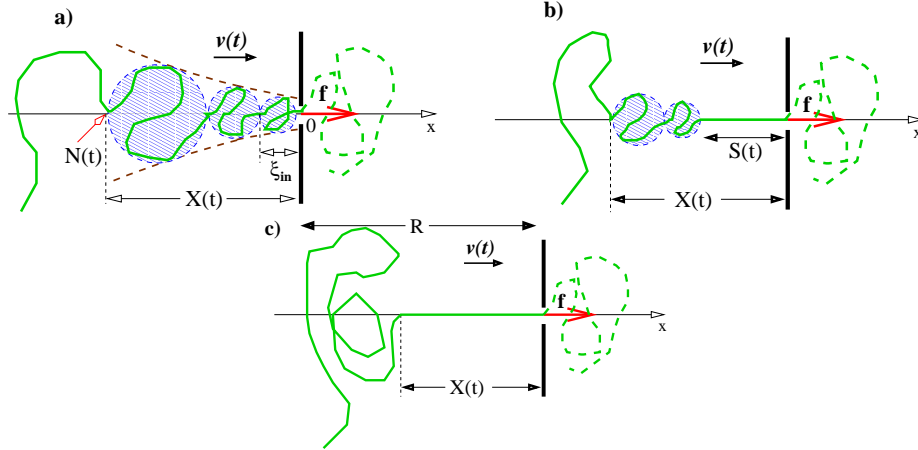


FIG. 1: (Color online) Dynamical response of the polymer chain shortly after the driving force f has been switched on. By the time t the tension is transmitted up to the $N(t)$ -th monomer. The number of the translocated monomers is denoted by $M(t)$ (indicated by a dashed line on the *trans*-side of the pore). The distance between the propagating tension front and the membrane is marked as $X(t)$. The portion of the chain marked as $X(t)$ is moving with an average time-dependent velocity $v(t)$. a) The “trumpet” regime at driving force $k_B T/aN^\nu \ll f \leq k_B T/a$. The initial blob size is $\xi_{in} = k_B T/f$. b) At $k_B T/a \leq f \ll (k_B T/a)N^\nu$ the part of the chain affected by tension starts as a “stem” of the length $S(t)$ and then turns into a “trumpet” (“stem-trumpet” regime). c) At $f > (k_B T/a)N^\nu$ the tensed part of the chain is completely stretched (“stem” regime). R marks the unperturbed chain size, i.e., $R = aN^\nu$.

Figure 1 shows schematically the case of *tensile force transmission*. The driving as well as the friction forces are x -dependent which leads for a relatively small driving force exerted on a segment in the pore, $k_B T/aN^\nu \ll f \leq k_B T/a$, to the so-called “trumpet” blob picture (shaded area in Fig. 1a) [20, 21]. By equating the local driving and drag forces (see Eq. (2.5)) and using the relationship between the tensile blob size $\xi(x)$ and the force $f(x)$ (cf. Eq. (2.4)), one could derive the “trumpet” profile equation (cf. Eq. (2.9)). The location of the tension front $X(t)$ is defined by the free boundary condition $f(x = -X(t)) = 0$. This condition along with the material balance Eq. (2.14) and the closure relation, Eq. (2.15), leads to the differential equation, Eq. (2.20), for the front propagation $X(t)$. The characteristic time of this transmission is given as $\tau_1 = C_1 N^{1+\nu}/f^{z-1-1/\nu}$ (cf. Eq. (2.23)), where the dynamical exponent $z = 2 + 1/\nu$ for the free-draining (or Rouse) case, and $z = 3$ for the non-draining (or Zimm) case, C_1 being

a model dependent constant. For a Rouse chain, $\tau_1 = C_1 N^{1+\nu}/f$ which agrees with the scaling law predicted by Kantor and Kardar [12]. During the process of tensile force transmission (or, front propagation), the velocity $v(t)$ of the moving domain decreases (because as time goes by more and more segments get incorporated in the moving domain) and at the time $t = \tau_1$ it approaches a stationary value v_s . After that a stationary regime sets in and the rest of the chain is sucked into the pore with a constant velocity v_s (cf. Eq. (2.24)). The characteristic time of this *stationary suction* process is $\tau_2 = C_2 N^{2\nu}/f^{z-2}$, (see Eq. (2.25)). The times τ_1 and τ_2 add up to a net translocation time $\langle\tau\rangle = \tau_1 + \tau_2$. Generally, the force transmission time τ_1 prevails for a strong enough driving force and a long chain (see Eq. (2.27)). Thus, the translocation time scaling ranges between $N^{2\nu}/f^{z-2}$ and $N^{1+\nu}/f^{z-1-1/\nu}$, depending on the pulling force intensity.

For moderate, $k_B T/a \leq f \ll (k_B T/a)N^\nu$, and strong, $(k_B T/a)N^\nu < f$, forces, the “trumpet” regime is replaced by the “stem-trumpet”, see Fig. 1b, and “stem”, see Fig. 1c, regimes respectively. In the “stem-trumpet” case, the part marked as $S(t)$ of the total moving domain looks like a stem whereas the rest resembles a trumpet shape. For the “stem” scenario of the force transmission the total moving domain looks like a completely stretched portion, see Fig. 1c. In both regimes the characteristic times of the force transmission and stationary suction into the pore are $\tau_1 \sim N^{1+\nu}/f$, and $\tau_2 \sim N^{2\nu}/f$. It could be seen that the time τ_1 dominates for a longer chain (see Eq. (2.45)). In the Table I we summarize the results of the theoretical scaling prediction for the translocation time $\langle\tau\rangle \propto N^\alpha f^{-\delta}$ (for the Rouse case) as well as the corresponding MD-simulation findings which will be discussed in this Sec. II and in Sec. III.

Regime	Exponents α and δ (theory)	Conditions	Exponents α and δ (MD)
Trumpet:	$\alpha = 2\nu \approx 1.18$, $\delta = 1/\nu \approx 1.66$ $\alpha = 1 + \nu \approx 1.59$, $\delta = 1$ see Eq. (2.26)	$\tilde{f}_R \ll (C_2/C_1)^{\nu/(1-\nu)}$ $\tilde{f}_R \gg (C_2/C_1)^{\nu/(1-\nu)}$ see Eq.(2.27)	$\alpha \approx 1.11$, $\delta \approx 1.17$ $\alpha \approx 1.47$, $\delta \approx 0.97$ see Sec. III
Stem-Trumpet and Stem:	$\alpha = 2\nu \approx 1.18$, $\delta = 1$ $\alpha = 1 + \nu \approx 1.59$, $\delta = 1$ see Eq. (2.44)	short chain longer chain see Eq.(2.45)	

TABLE I: Exponents α and δ for the translocation time scaling $\langle\tau\rangle \propto N^\alpha f^{-\delta}$ in the free-draining (Rouse) case as predicted by the theory (theory) and by our MD-simulation (MD) (see Sec. III). The parameter $\tilde{f}_R \stackrel{\text{def}}{=} aN^\nu f/k_B T$, whereas C_1 and C_2 are some numerical model-dependent parameters.

Schematically, our theoretical findings for the scaling behavior of $\langle\tau\rangle$ for the “trumpet” regime (see Sec. IIC) are plotted in Fig. 2a (for $\langle\tau\rangle \sim N^\alpha$) and in Fig.2b (for $\langle\tau\rangle \sim f^{-\delta}$). The time evolution of the number of translocated monomers $M(t)$ is also investigated in Sec. IIC2. Again, depending on driving force intensity, the $M(t)$ vs. time t scaling law changes, see Fig.2c, from $M(t) \propto (ft)^{1/(1+\nu)}$ (at strong force, when the force transmission dominates) (see Eq. (2.30)) to $M(t) \propto (ft)/N^\nu$ (for weak force, when the stationary suction process dominates and $t \ll \tau_2$) (see Eq. (2.34)). These $M(t)$ vs. t dependencies clearly illustrate the presence of an initial stage, which in the Sec. IIB is called *blob initiation*, and is confirmed by our MD-results (see Fig. 7 where the translocation coordinate $\langle s \rangle \stackrel{\text{def}}{=} M(t)$ vs. time t is given). It will also be shown that the characteristic time of this initial stage τ_{init} changes with force as $\tau_{\text{init}} \sim 1/f$ (see Eq. (2.2) and Fig. 8).

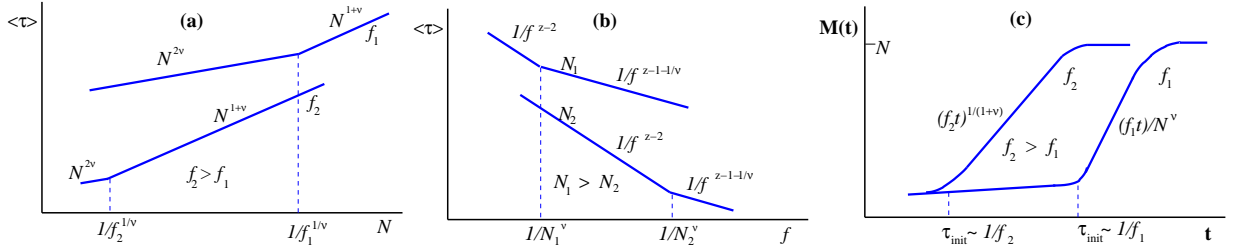


FIG. 2: Schematic representation of the main scaling predictions: a) Translocation time $\langle\tau\rangle$ vs. chain length N at a fixed force f . With growing force $\tilde{f}_R \stackrel{\text{def}}{=} aN^\nu f/k_B T$ the scaling law $\langle\tau\rangle \sim N^\alpha$ changes from $\langle\tau\rangle \sim N^{2\nu}$ to $\langle\tau\rangle \sim N^{1+\nu}$. b) Translocation time $\langle\tau\rangle$ vs. driving force f at different chain lengths $N_1 > N_2$. c) Translocation length $M(t)$ vs. time t for two different forces $f_2 > f_1$. The characteristic time for initial blob formation goes as $\tau_{\text{init}} \sim 1/f$.

We will devote the rest of this Sec. II to the detailed discussion of the “trumpet”, “stem-trumpet” and “stem” regimes as well as to the mean translocation length $M(t)$ behavior. Readers who are not interested in the mathematical

aspects of the problem can skip these details and go to Sec. III. One should keep in mind, however, that before one or another type of tensile force transmission comes into play, an initial blob should always set in.

B. Blob initiation

The starting deformation (i.e., *blob initiation*) of a polymer chain that has been initially at rest and is then pulled by a force f constitutes a necessary stage to set in the driving force transmission. An initial blob of size $\xi_{\text{init}} = k_B T / f$ is formed which contains g beads so that $\xi_{\text{init}} = a g^\nu$ where a is the Kuhn segment length and ν is the Flory exponent, mentioned above. Denote $\tau_0 = a^2 \zeta_0 / k_B T$ as the characteristic diffusion time of a single bead with ζ_0 being the Stokes friction coefficient [22]. Then the blob initiation time can be written in the scaling form

$$\tau_{\text{init}} = \tau_0 \phi \left(\frac{\xi_{\text{init}}}{a} \right) \quad (2.1)$$

so that the scaling function $\phi(y)$ depends only on the dimensionless combination ξ_{init}/a (i.e., on the size of the blob itself). On the other hand, we assume that the initial blob formation happens due to purely mechanical traction which almost does not affect the chain meanders. This is supported by the fact that within the time interval $0 < t < \tau_{\text{init}}$ only few segments are translocated (see Fig. 2c). Thus, the characteristic time τ_{init} does not depend on temperature T and is determined only by the Stokes friction coefficient ζ_0 and the pulling force f . Since $\tau_0 \propto 1/k_B T$, this implies $\phi(y) \propto y$, and one gets as a result

$$\tau_{\text{init}} = \left(\frac{a^2 \zeta_0}{k_B T} \right) \left(\frac{k_B T}{a f} \right) \propto \frac{\zeta_0 a}{f} \quad (2.2)$$

The rearrangement of the initial blob leads at $t > \tau_{\text{init}}$ to a subsequent tensile force transmission which is governed by the local balance of driving and drag forces. The blob initiation characteristic time τ_{init} is indeed clearly seen in our MD-simulation results (see Fig.7) and found to change as $\sim 1/f$. In the next sections we consider different regimes of this tensile force transmission, depending of the strength of f , which are named after some characteristic shapes of the resulting chain conformation.

C. Trumpet regime

In this case the driving force is moderately strong and falls within the range

$$\frac{k_B T}{a N^\nu} \ll f \leq \frac{k_B T}{a} \quad (2.3)$$

Schematically, a typical conformation of a driven polymer in the trumpet regime is represented by the shaded area in Fig. 1. At a given time t some fraction of the chain is subjected to tension. This part of the chain comprises a sequence of Pincus blobs of different size,

$$\xi(x) = \frac{k_B T}{f(x)}, \quad (2.4)$$

where $f(x)$ is the local (i.e. x -dependent) value of the driving force. As is evident from Fig. 1, the blob size at a given position x corresponds to the lateral chain meandering at x . According to the blob definition $\xi(x) = a g(x)^\nu$ where $g(x)$ is the number of beads in the blob (we recall that the chain inside the blob follows Self Avoiding Walk - statistics). On the other hand, as stipulated by the local force balance, the driving force equals the friction (Stokes) force, i.e.

$$f(x) = \zeta_0 v(t) \int_{-X(t)}^x \left[\frac{\xi(x')}{a} \right]^{z-2} \frac{dx'}{\xi(x')} \quad (2.5)$$

In Eq.(2.5) we take into account that $dx'/\xi(x')$ is the number of blobs on the interval $\{x', x' + dx'\}$ whereas $\zeta_0 v(t) [\xi(x')/a]^{z-2}$ is the local Stokes friction force. The dynamical exponent z in Eq. (2.5), which determines

the total number of monomers in this portion of the chain, is $z = 2 + 1/\nu$ for the case of Rouse dynamics, and $z = 3$ for the Zimm statistics [22]. Thus, taking into account Eq. (2.4), the expression for the blob size becomes

$$\xi(x) = \frac{k_B T}{\zeta_0 v(t) \int_{-X(t)}^x [\xi(x')/a]^{z-2} dx' / \xi(x')} , \quad (2.6)$$

or, represented in a differential form,

$$\frac{d\xi}{dx} = - \frac{\zeta_0 v(t)}{k_B T a^{z-2}} \xi^{z-1} \quad (2.7)$$

Eq. (2.7) should be supplemented by the boundary condition

$$\xi(x = -k_B T/f) = \xi_{\text{init}} = \frac{k_B T}{f} \quad (2.8)$$

which represents the initial blob in the 'trumpet' (cf. Fig. 1). Then, the solution of Eq. (2.7) takes on the form

$$\xi(x) = a \left[\frac{\zeta_0 v(t)}{k_B T} \left(x + \frac{k_B T}{f} \right) + \left(\frac{af}{k_B T} \right)^{z-2} \right]^{1/(2-z)} \quad (2.9)$$

where in the case of Rouse dynamics $z - 2 = 1/\nu$.

One can fix the blob size by the requirement that the force at the free boundary, i.e., at $x = -X(t)$, is equal to zero. Therefore,

$$f(x = -X(t)) = \frac{k_B T}{\xi(x = -X(t))} = 0 , \quad (2.10)$$

or, in view of Eq. (2.9), this yields $(\zeta_0 v/k_B T)(-X(t) + k_B T/f) + (af/k_B T)^{z-2} = 0$. Solving the latter for $X(t)$,

$$X(t) = \frac{k_B T}{f} + \frac{k_B T}{\zeta_0 v(t)} \left(\frac{af}{k_B T} \right)^{z-2} , \quad (2.11)$$

one may exclude f in Eq. (2.9) in favor of $X(t)$. As a result we have

$$\xi(x) = \frac{a}{[\zeta_0 v(t) (x + X(t))/k_B T]^{1/(z-2)}} \quad (2.12)$$

The largest blob of size $\xi_X(t)$ in the trumpet is placed at $x = -X(t) + \xi_X(t)$. From Eq. (2.12) one immediately obtains

$$\xi_X(t) = a \left[\frac{k_B T}{\zeta_0 a v(t)} \right]^{1/(z-1)} \quad (2.13)$$

We are now in a position to derive the differential equation for the location of the tension front $X(t)$. To this end we use the material balance equation (mass conservation law). Let the tension be transmitted up to the $N(t)$ -th monomer whereas $M(t)$ denotes the number of translocated monomers (see Fig. 1). Then the material balance equation reads

$$\int_{-X(t)}^0 \left[\frac{\xi(x)}{a} \right]^{1/\nu} \frac{dx}{\xi(x)} + M(t) = N(t) \quad (2.14)$$

where the first integral yields the number of monomers in the shaded portion of the chain (see Fig.1).

Denote the total number of monomers that has been subjected to tension during the time interval $\{0, t\}$ by $N(t)$. At $t = 0$ all these $N(t)$ monomers have been in equilibrium occupying a region of average size $X(t)$. Therefore $N(t)$ and $X(t)$ are related by the Flory expression, i.e.,

$$X(t) = aN(t)^\nu , \quad (2.15)$$

which will be used below as a closure relation.

The local density in the moving domain of blobs (shaded portion in Fig. 1) is $\rho(x) \simeq g(x)/\xi(x)^3$ whereas the cross-section area is locally $\Sigma(x) \simeq \xi(x)^2$. The smallest blob next to the membrane orifice seeps through the pore into the *trans*-side of space so that the number of translocated monomers can be calculated[15] as

$$\begin{aligned} M(t) &= \int_0^t \rho(x)\Sigma(x)|_{x=0} v(t') dt' = \int_0^t \left[\frac{\xi(x=0)}{a} \right]^{1/\nu} \frac{1}{\xi(x=0)} v(t') dt' \\ &= \frac{1}{\tau_0} \int_0^t [\tilde{v}(t')]^{1-\frac{1-\nu}{\nu(z-2)}} [\tilde{X}(t')]^{-\frac{1-\nu}{\nu(z-2)}} dt' \end{aligned} \quad (2.16)$$

where we have used Eq. (2.12) for the blob size and have introduced the bead characteristic time $\tau_0 = a^2\zeta_0/k_BT$ as well as the dimensionless (tilded) variables [16]: $\tilde{v}(t) = \zeta_0 a v(t)/k_BT$ and $\tilde{X}(t) = X(t)/a$. Moreover, using Eq. (2.11) we can exclude $\tilde{v}(t')$ in favor of $\tilde{X}(t)$ and the dimensionless force $\tilde{f}_a = af/k_BT$. As a result

$$M(t) = \tilde{f}_a^{z-1-1/\nu} \frac{1}{\tau_0} \int_0^t \frac{dt'}{\tilde{X}(t') \left[1 - 1/\tilde{f}_a \tilde{X}(t') \right]^{1-\frac{1-\nu}{\nu(z-2)}}} \quad (2.17)$$

Now we use Eqs. Eq. (2.11) and (2.12) to determine the first integral-term in Eq. (2.14) where we also take into account Eq. (2.17) and the closure Eq. (2.15). As a result, the material balance condition Eq. (2.14) takes on the form

$$\tilde{X}(t) \left[1 - \frac{1}{\tilde{f}_a \tilde{X}(t)} \right]^{\frac{1-\nu}{\nu(z-2)}} \tilde{f}_a^{1-\frac{1}{\nu}} + \tilde{f}_a^{z-1-\frac{1}{\nu}} \frac{1}{\tau_0} \int_0^t \frac{dt'}{\tilde{X}(t') \left[1 - \frac{1}{\tilde{f}_a \tilde{X}(t')} \right]^{1-\frac{1-\nu}{\nu(z-2)}}} = [\tilde{X}(t)]^{\frac{1}{\nu}} \quad (2.18)$$

For relatively long time intervals $\tilde{f}_a \tilde{X}(t) \gg \tilde{f}_a \simeq 1$ and Eq. (2.18) takes on the form

$$\tilde{X}(t) \tilde{f}_a^{1-\frac{1}{\nu}} + \tilde{f}_a^{z-1-\frac{1}{\nu}} \frac{1}{\tau_0} \int_0^t \frac{dt'}{\tilde{X}(t')} = [\tilde{X}(t)]^{\frac{1}{\nu}} \quad (2.19)$$

Differentiation of Eq. (2.19) with respect to time yields a differential equation for $\tilde{X}(t)$

$$\tau_0 \left[1 - B_0 \left(\tilde{f}_a \tilde{X}(t) \right)^{1/\nu-1} \right] \frac{d\tilde{X}(t)}{dt} = -\frac{\tilde{f}_a^{z-2}}{\tilde{X}(t)} \quad (2.20)$$

where B_0 is a constant of the order of unity. Eq.(2.20) should be supplemented by the initial condition

$$\tilde{X}(t=0) = \tilde{\xi}_{\text{in}} = \frac{1}{\tilde{f}_a} \quad (2.21)$$

which simply indicates that the force transmission starts right after the initial blob has formed as we have discussed in Sec. IIA. The solution of Eq. (2.20) has the following form

$$t = t_0 + \tau_0 B_0 \tilde{f}_a^{1/\nu-z+1} \tilde{X}(t)^{1/\nu+1} \{ 1 - C_0 / [\tilde{f}_a \tilde{X}(t)]^{1/\nu-1} \} \quad (2.22)$$

where $C_0 = 1/B_0$ and $t_0 = \tau_0(1 - B_0)/\tilde{f}_a^z$. The characteristic time τ_1 for the last monomer to attain its steady state follows from $\tilde{X}(\tau_1) = N^\nu$ which, due to Eq. (2.22), yields

$$\tau_1 = \tau_0 B_0 \tilde{f}_a^{1/\nu-z+1} N^{1+\nu} \left[1 - C_0 / \tilde{f}_R^{1/\nu-1} \right] \quad (2.23)$$

where N is the total chain length, $\tilde{f}_R = Rf/k_BT$ and $R = aN^\nu$ stands for the unperturbed chain size.

1. Stationary part of the translocation: suction into the pore

The stationary regime sets in within a characteristic time τ_1 . After that the non-translocated part of the chain, $N - M(\tau_1)$, is pulled as a whole entity towards the pore (suction). The stationary velocity v_s is defined from Eq. (2.11) by putting $\tilde{X}(\tau_1) = N^\nu$. As a result for $\tilde{f}_a \tilde{X}(\tau_1) \gg 1$ we have

$$\tilde{v}_s = \frac{1}{N^\nu} \tilde{f}_a^{z-2} \quad (2.24)$$

where the dimensionless velocity $\tilde{v}_s = \zeta_0 a v_s / k_B T$. The characteristic time for the stationary part of translocation is then derived as

$$\tau_2 = \tau_0 \frac{\tilde{X}(\tau_1)}{\tilde{v}_s} = \tau_0 \frac{N^{2\nu}}{\tilde{f}_a^{z-2}} \quad (2.25)$$

Eventually, the total translocation time $\langle \tau \rangle$ can be seen as a sum of τ_1 and τ_2 . Thus, by taking into consideration Eq. (2.23) (at $\tilde{f}_R \gg 1$) and Eq. (2.25) we derive one of our main results,

$$\langle \tau \rangle = \tau_0 C_1 \tilde{f}_a^{1/\nu-z+1} N^{1+\nu} + \tau_0 C_2 \tilde{f}_a^{2-z} N^{2\nu} \quad (2.26)$$

where C_1 and C_2 are some numerical model dependent constants. The first term in Eq. (2.26) dominates in case $C_1 \tilde{f}_a^{1/\nu-z+1} N^{1+\nu} \gg C_2 \tilde{f}_a^{2-z} N^{2\nu}$, that is, for sufficiently large driving forces f and moderate chain lengths N , or, alternatively for very long chains even if the driving force is rather weak:

$$\tilde{f}_R \gg (C_2/C_1)^{\nu/(1-\nu)} \quad (2.27)$$

where $\tilde{f}_R = a N^\nu f / k_B T$. The combined schematic representation of the scaling law, Eq. (2.26), as well as the criterion given by Eq. (2.27) is given in Table I and in Fig. 2a, b.

The central result given by Eq. (2.26) predicts a scaling relation for the mean translocation time $\langle \tau \rangle \propto N^\alpha f^{-\delta}$ with a force-dependent exponent α that grows from 2ν to $1 + \nu$ as the parameter $a N^\nu f / k_B T$ increases. Numerical results obtained by means of Langevin Dynamics (LD) simulation in two dimensions (2D) clearly support this behavior: one observes $\alpha = 1.50$ for relatively short chains ($N \leq 200$) and $\alpha = 1.69$ for longer chains [23]. In three dimensions (3D) there is no clear evidence of such crossover. In the total interval of chain lengths which was studied in 3D the exponent $\alpha = 1.41$ [23] and $\alpha = 1.36$ [24], i.e. the exponent value falls in the range between 2ν and $1 + \nu$. In a series of LD simulation studies by Lehtola et al. [25–27] it was found (within chain length interval $N \leq 800$) that α systematically increases with f up to roughly $\alpha = 1 + \nu$. This is in agreement with our theoretical and MD-results (see below Sec. III) but is in clear contradiction to the results of K. Luo et al. [28] where the exponent $\alpha = 1 + \nu \approx 1.59$ was found for relatively short chains, $N \leq 200$ and for small driving forces. Moreover, the exponent α becomes smaller, $\alpha \approx 1.37$ as the driving force grows. Experimentally, the scaling law $\langle \tau \rangle \propto N^{2\nu}/f$, which follows from Eq. (2.26) for relatively weak forces \tilde{f}_R and $z = 3$ (Zimm dynamics), has been found in ref. [29, 30] in the case of synthetic pore. Recently the scaling given by the first term in Eq. (2.26) has been obtained in ref. [9] using the so-called “iso-flux trumpet” model (which was also inspired by the Sakaue’s paper).

Eventually, we should like to point out that the first term of Eq. (2.26) (which corresponds to the characteristic time of tensile force transmission) *differs* from the corresponding term given by Eq. (10) in ref.[16]. This difference arises even if one assumes, following Sakaue’s idea, that the entire trumpet is characterized by a single time dependent velocity (“iso-velocity trumpet”!). The reason for this discrepancy is discussed in the Appendix A.

2. Time evolution of the translocated portion $M(t)$

The number of translocated monomers $M(t)$, given by Eq. (2.17), grows with elapsed time. In the case when the second term in Eq. (2.22) dominates, one gets

$$t \simeq \tau_0 B_0 \tilde{f}_a^{1/\nu-z+1} \tilde{X}(t)^{1/\nu+1} \quad (2.28)$$

Combining this equation with Eq. (2.17) (where again we assume $\tilde{f}_a \tilde{X}(t) \gg 1$), one arrives at

$$M(t) = (\tilde{f}_a)^x \int_0^{t/\tau_0} (\tilde{t})^{-\frac{\nu}{1+\nu}} d\tilde{t} = C_0 (\tilde{f}_a)^x (\tilde{t})^{1/(1+\nu)} \quad (2.29)$$

where the exponent $\chi = (z\nu - 1 - \nu)/\nu(1 + \nu)$. In the case of Rouse dynamics $z\nu = 2\nu + 1$ and $\chi = (1 + \nu)^{-1}$. The resulting translocation relationship can be written as

$$M(t) = c_0 \left(\tilde{f}_a \tilde{t} \right)^{1/(1+\nu)} \quad (2.30)$$

As far as mean translocation time $\langle \tau \rangle$ should satisfy the requirement $M(\langle \tau \rangle) = N$, one recovers the result $\langle \tau \rangle \simeq \tau_0 N^{1+\nu}/f$ (see Eq. (2.26)).

In the case of small driving force, $\tilde{f}_a N^\nu \simeq 1$ and $\tilde{f}_a N^\nu \ll (C_2/C_1)^{\nu/(1-\nu)}$, the translocation process is mainly determined by the stationary suction into the pore whereby the translocation time $\langle \tau \rangle \simeq C_2 \tau_0 N^{2\nu}/\tilde{f}_a^{z-2}$. On the other hand, the number of translocated monomers according to Eq. (2.16) reads

$$M(t) = \tilde{v}_s \int_0^t \left[\frac{\xi(x=0)}{a} \right]^{1/\nu} \frac{1}{\xi(x=0)} dt = [\tilde{v}_s]^{1-\frac{1-\nu}{\nu(z-2)}} \frac{1}{\tau_0} \int_0^t \frac{dt'}{[\tilde{X}(t')]^{\frac{1-\nu}{\nu(z-2)}}} \quad (2.31)$$

where we have used the expression for the blob size Eq. (2.12) with the stationary velocity \tilde{v}_s . In the stationary regime the size of the moving domain has the form $\tilde{X}(t) = \tilde{X}(\tau_1) - \tilde{v}_s t/\tau_0 \simeq N^\nu - \tilde{v}_s t/\tau_0$. By making use of this in Eq. (2.31) and after integration, we arrive at the result

$$M(t) = \frac{N^\nu}{\tilde{f}_a^{(1-\nu)/\nu}} \left\{ 1 - \left[1 - \frac{t}{\tau_2} \right]^{1-\frac{1-\nu}{\nu(z-2)}} \right\} \quad (2.32)$$

Consider first the large time limit $t \simeq \tau_2$. In this case $M(\tau_2) \simeq N$ and the Eq. (2.32) leads us back to the condition $\tilde{f}_a N^\nu \simeq 1$. At $t \ll \tau_2$ the expansion in Eq. (2.32) suggests that

$$M(t) \simeq c_1 \frac{\tilde{f}_a^{z-1-1/\nu}}{N^\nu} \tilde{t} \quad (2.33)$$

where, as before, $\tilde{t} = t/\tau_0$. In the case of Rouse dynamics we finally obtain

$$M(t) \simeq \frac{c_1}{N^\nu} \tilde{f}_a \tilde{t} \quad (2.34)$$

As can be seen from Eq. (2.34), the formal extrapolation the linear time dependence law up to the final time t_f (where $M(t_f) \simeq N$) gives $t_f \propto N^{1+\nu}/\tilde{f}_a \simeq \tau_1 \ll \tau_2$. As a consequence, a sub-linear slowing down behavior should be seen at a later time interval. The two regimes mentioned above (i.e., for strong and weak driving forces) are illustrated in Fig. 2c.

D. “Stem” and “stem-trumpet” scenario

1. Stem

The above consideration is valid in the range of forces given by Eq. (2.3). For stronger forces which are within the range

$$1 \leq \tilde{f}_a \ll N^\nu \quad (2.35)$$

the tensile force transmission follows the so called *stem-trumpet* scenario [20, 21], as indicated in Fig. 1b, whereby the part of the polymer chain that is close to the membrane attains a completely stretched conformation.

Consider first the limit of very strong force $\tilde{f}_a > N^\nu$ where the configuration is depicted by the *stem* picture shown in Fig. 1c. In this case the force balance reads

$$\tilde{v}(t)\tilde{X}(t) = \tilde{f}_a \quad (2.36)$$

The material balance (cf. Eq. (2.14)) yields

$$\tilde{X}(t) + M(t) = N(t) \quad (2.37)$$

The number of translocated segments (cf. Eq.(2.16)) is

$$M(t) = \frac{1}{a} \int_0^t v(t') dt' = \frac{1}{\tau_0} \int_0^t \tilde{v}(t') dt' \quad (2.38)$$

With the help of Eqs. (2.36), (2.37) and (2.38) as well as using the closure Eq. (2.15) one finds

$$\tilde{X}(t) + \frac{\tilde{f}_a}{\tau_0} \int_0^t \frac{dt'}{\tilde{X}(t')} = [\tilde{X}(t)]^{1/\nu} \quad (2.39)$$

In differential form this equation reads

$$\tau_0 \left\{ C_0 [\tilde{X}(t)]^{1/\nu} - C_1 \tilde{X}(t) \right\} \frac{d\tilde{X}}{dt} = \tilde{f}_a \quad (2.40)$$

with an initial condition $\tilde{X}(t=0) = 1$ and C_0 , and C_1 being some constants. The corresponding solution of Eq. (2.40) is given by

$$\frac{\tilde{f}_a}{\tau_0} t - \tilde{C}_1 + \tilde{C}_0 = \tilde{C}_0 [\tilde{X}(t)]^{1/\nu+1} \left\{ 1 - \frac{\tilde{C}_1}{\tilde{C}_0 [\tilde{X}(t)]^{1/\nu-1}} \right\} \quad (2.41)$$

Again the characteristic time τ_1 is defined as $\tilde{X}(\tau_1) = \tilde{R} = N^\nu$. Then, for the reasonably long chains $N^{1-\nu} \gg \tilde{C}_1/\tilde{C}_0$ the first terms in Eq.(2.41) prevails. As a result, the characteristic time τ_1 is obtained as

$$\tau_1 = \tau_0 \frac{N^{1+\nu}}{\tilde{f}_a} \quad (2.42)$$

As before, the second (stationary) stage of the translocation is related to the pulling force by considering this part of the chain as an entity which moves with stationary velocity $\tilde{v}_s = \tilde{f}_a/N^\nu$. The corresponding characteristic time τ_2 is given by

$$\tau_2 = \tau_0 \frac{\tilde{R}}{\tilde{v}_s} = \tau_0 \frac{N^{2\nu}}{\tilde{f}_a} \quad (2.43)$$

Therefore, the total translocation time $\langle \tau \rangle$ is a combination of τ_1 and τ_2 , i.e.,

$$\langle \tau \rangle = C_1 \tau_0 \frac{N^{1+\nu}}{\tilde{f}_a} + C_2 \tau_0 \frac{N^{2\nu}}{\tilde{f}_a} \quad (2.44)$$

The first term in Eq. (2.44) dominates at

$$N^{1-\nu} \gg C_2/C_1 \quad (2.45)$$

i.e., for a reasonably long chains. One should note that in this limit we recover the scaling law of the trumpet regime, provided Eq. (2.45) holds and $\tilde{X}(t) = (\tilde{f}_a \tilde{t})^{\nu/(1+\nu)}$. The velocity $\tilde{v}(t) = \tilde{f}_a/\tilde{X}(t) = \tilde{f}_a(\tilde{f}_a \tilde{t})^{-\nu/(1+\nu)}$, and the number of translocated monomers is obtained as

$$M(t) = \frac{1}{a} \int_0^t \tilde{v}(t') dt' \simeq B_0 \left(\tilde{f}_a \tilde{t} \right)^{1/(1+\nu)} \quad (2.46)$$

whereby one goes back to Eq. (2.30).

2. The Stem-trumpet regime

In the interval of force strengths, Eq. (2.35), the chain deformation starts with the formation of a stem whereby the velocity changes as

$$\tilde{v}(t) \simeq \left(\tilde{f}_a\right)^{1/(1+\nu)} \left(\frac{\tau_0}{t}\right)^{\nu/(1+\nu)} \quad (2.47)$$

Thus, the velocity decreases with time and at some moment $t \simeq \tau^\#$ the drag force at the stem-trumpet junction becomes comparable to $k_B T/a$, i.e., $\zeta_0 v(\tau^\#) \simeq k_B T/a$. Therefore,

$$\tau^\# \simeq \tau_0 (\tilde{f}_a)^{1/\nu} \quad (2.48)$$

At $t > \tau^\#$ the stem-trumpet picture dominates. For the blob size of the flower (trumpet) part the same differential equation Eq. (2.7) holds. However, the boundary conditions (BC) are different. Namely, in this case $\xi(x = -S(t)) = a$ and the solution of Eq.(2.7) yields $\xi(x) = a \{1 + \zeta_0 v(t)[x + S(t)]/T\}^{1/(2-z)}$. Therefore, the solution is given in the total x -interval by

$$\xi(x) = \begin{cases} a \{1 + \zeta_0 v(t)[x + S(t)]/k_B T\}^{1/(2-z)} & , \text{ for } -X(t) \leq x \leq -S(t) \\ a & , \text{ for } -S(t) \leq x \leq 0 \end{cases} \quad (2.49)$$

For $x = -X(t)$ the force vanishes, i.e., $f(x = -X(t)) = T/\xi(x = -X(t)) = 0$, and one has

$$X(t) = S(t) + \frac{k_B T}{\zeta_0 v(t)} \quad (2.50)$$

The material balance may be written as

$$\int_{-X(t)}^{-S(t)} \left[\frac{\xi(x)}{a} \right]^{1/\nu} \frac{dx}{\xi(x)} + \frac{1}{a} S(t) + M(t) = N(t) \quad (2.51)$$

By making use of Eqs. (2.15), (2.49) and (2.50) in Eq. (2.51), one arrives at

$$\tilde{X}(t) + \frac{1}{a} \int_0^t v(t') dt' = [\tilde{X}(t)]^{1/\nu} \quad (2.52)$$

In order to exclude the velocity from Eq. (2.52) we should note that the tensile force at $x = -S(t)$ (junction point between “stem” and “trumpet”) is given by

$$f(x = -S(t)) = \frac{k_B T}{a} \quad (2.53)$$

Then the force balance for the stem can be written as

$$\zeta_0 v(t) \left[\frac{S(t)}{a} \right] = f - f(x = -S(t)) = f - \frac{k_B T}{a} , \quad (2.54)$$

and consequently,

$$\tilde{S}(t) = \frac{1}{\tilde{v}(t)} (\tilde{f}_a - 1) \quad (2.55)$$

This equation together with Eq. (2.50) yields

$$\tilde{X}(t) = \frac{1}{\tilde{v}(t)} \tilde{f}_a \quad (2.56)$$

and one retrieves the corresponding equation Eq.(2.36) for the stem case. Now, using Eq. (2.56) in Eq. (2.52) one arrives at the differential equation for $\tilde{X}(t)$

$$\tau_0 \left\{ B_0 [\tilde{X}(t)]^{1/\nu} - B_1 \tilde{X}(t) \right\} \frac{d\tilde{X}(t)}{dt} = \tilde{f}_a \quad (2.57)$$

which is again equivalent to Eq. (2.40) for the “stem” case. As a consequence, the expressions for the translocation time and $M(t)$ are given by Eqs. (2.44) and (2.46) respectively.

The main conclusion of this Sec. IID lies in the fact that for the moderate and strong forces the translocation exponent changes from $\alpha = 2\nu$ for moderately long chains to $\alpha = 1 + \nu$ for very large values of N . This is in good correspondence with the results of the Monte Carlo investigation [31].

III. NUMERICAL VERIFICATION OF THEORETICAL PREDICTIONS

A. Model

In order to verify the predictions of Section II we performed numerical simulations. The model assumes Langevin dynamics of a polymer chain which consists of N beads that thread through an octagonal pore through a closely-packed wall (membrane). The interaction between the monomers of the chain is modeled by a Finitely Extensible Nonlinear Elastic (FENE) springs corresponding to a pair potential

$$U_{FENE}(r_{ij}) = -\frac{kr_{ij}^2}{2} \ln \left(1 - \frac{r_{ij}^2}{R_0^2} \right), \quad (3.1)$$

where r_{ij} is the bond length between two beads and $R_0 = 1.5$ is the maximal bond length. All beads experience excluded volume interactions which are modeled by the repulsive part of the shifted Lennard-Jones potential, also

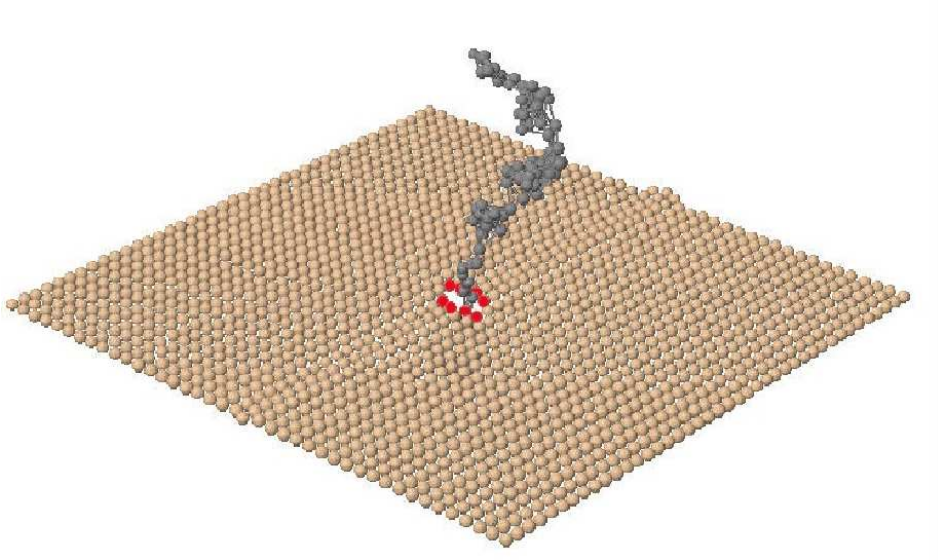


FIG. 3: (Color online) A snapshot configuration during translocation of the polymer chain. The nanopore is created by removing 8 beads, so that an octagonal hole results.

known as the Weeks-Chandler-Anderson (WCA) potential. This potential U_{WCA} is defined by

$$U_{WCA}(r_{ij}) = 4\epsilon \left[\left(\frac{\sigma}{r_{ij}} \right)^{12} - \left(\frac{\sigma}{r_{ij}} \right)^6 + \frac{1}{4} \right] \Theta(r_c - r), \quad (3.2)$$

where $\Theta(x)$ is the Heavyside-function, i.e., we use a cut-off $r_c = 2^{-1/6}\sigma$, implying $U_{WCA} = 0$ for $r_{ij} > r_c$. The monomers residing inside the pore experience a constant external force f in the direction perpendicular to the membrane, which we designate by x . The external force can be implemented by adding a linear potential U_{ext} , whose

value is 0 outside the pore and $f x$, if x is inside the pore region. Thus, f pulls the chain towards the region of positive x which we refer to as the *trans*-side. The equation of motion for the beads of the chain reads

$$m \frac{d^2 \mathbf{r}_i}{dt^2} = -\nabla (U_{FENE} + U_{LJ} + U_{ext}) - \gamma \frac{d\mathbf{r}_i}{dt} + \mathcal{R}_i(t), \quad (3.3)$$

where $\mathcal{R}_i(t)$ stands for a Brownian random force whose moments obey $\langle \mathcal{R}_i(t) \rangle = 0$ and $\langle \mathcal{R}_i^\alpha(t_1) \mathcal{R}_j^\beta(t_2) \rangle = 2k_B T \gamma \delta(t_1 - t_2) \delta_{\alpha,\beta} \delta_{i,j}$. The parameter values were set to $\epsilon = 1.2$, $\sigma = 1.0$, $k = 60.0$, $\gamma = 0.73$ and were kept fixed during the simulations. The temperature had a constant value given by $T = 1.2\epsilon/k_B$. These parameters correspond to the model used in the ref.[27].

The membrane is modeled by a plane of beads whose positions are kept fixed. Eight neighboring monomers are removed to obtain an octagonal pore. The interaction between the beads of the chain and the plane is mediated through the repulsive WCA potential. All simulations were performed starting from a configuration in which initially all beads except the first one were on the *cis*-side. The chain is fully translocated when all beads have made their way to the *trans*-side. To prevent the chain from retracting to the *cis*-side, reflecting boundary conditions were imposed on the first monomer on the chain by making its size larger than the pore diameter. A typical configuration for a polymer with $N = 100$ in 3D is shown in Fig. 3.

B. Results

To check the validity of the blob picture, derived in Sec. II, we start by preparing contour plots of the monomer density. We assume that the chain propagates in the positive x -direction, that is, perpendicular to the membrane; the z -direction is parallel to the membrane and equivalent to the y . The contour plots of the density distribution Figs. 4a - 4d describe the change in the average polymer conformation at different stages of the translocation process.

In order to gain more insight into the translocation process we have also plotted similar data in a different form. Figure 5 demonstrates the density profiles (normalized to unity) in x -direction for different time moments. This representation clearly shows that the tensile force transmission (or front propagation) in x -direction (as it was described in Sec. IIC) is really visible. Namely, the moving domain grows at the expense of the rear part of the chain which is still at rest. After approximate time $t = 70000$, the non-translocated part of the chain moves as a whole (cf. Sec. IIC1, where this second stage of translocation was qualified as the “suction into the pore”).

Figure 5 also clearly shows the presence of “crowding” effect, i.e., a fairly strong compression of the coil on the *trans*-side in x -direction (i.e. at $x > 0$). This effect results from the fact that the characteristic time τ of a forced translocation (which ranges, as we have shown in Sec. IIC, between $\tau_1 \sim N^{1+\nu}$ and $\tau_2 \sim N^{2\nu}$), is by all means much smaller than the characteristic Rouse time $\tau_R \sim N^{2\nu+1}$, that is, the threaded beads on the *trans*-side fail to disperse and form an equilibrated coil conformation in an interval $\tau < \tau_R$. This crowding effect has been discussed recently in more detail [32] and it was shown that immediately after translocation an effective Flory exponent $\nu_{eff} = 0.45$ is observed, i.e., ν_{eff} is smaller than $\nu = 0.59$ for a chain in equilibrium.

1. Scaling of the translocation time

In Sec. IIC we have shown that the time for a driven translocation scales as $\langle \tau \rangle \sim N^\alpha f^{-\delta}$. For large forces (the corresponding condition is given by Eq. (2.27)) the translocation exponent $\alpha = 1 + \nu \approx 1.59$ and $\delta = 1$ (for the so-called free-draining or Rouse dynamics). Thus one goes back to the scaling relationship, predicted first by Kantor and Kardar [12]. Very recently [9] the same scaling has been obtained on a basis of the so-called “iso-flux trumpet” consideration. In fact, in this case the translocation time is determined by the propagation of tensile force with characteristic time τ_1 given by Eq. (2.23). At relatively small forces, in contrast, the exponents are predicted to be $\alpha = 2\nu \approx 1.18$, and $\delta = 1/\nu \approx 1.7$ (“trumpet” regime), or $\delta = 1$ (“stem-trumpet” regime). At small forces the process is dominated by stationary suction of the rest of the chain after the force transmission stage.

The results for the $\langle \tau \rangle$ vs. N scaling relationship at different driving forces, derived from our MD-simulation, are shown in Fig. 6a. We performed numerical simulations for chains with lengths $N = 40, 70, 100, 200, 300, 500$ and forces 1, 2, 5, 10, 20. For every set of parameters at least 1000 runs were performed, and most averages were obtained from 3000 separate runs. The $N = 500$ runs took a long time, mostly because relaxation to equilibrium (as a starting condition) was very time consuming. The $f = 1, 2$ results for the $N = 500$ chain are therefore typically averaged over 1000 runs. It can be seen from Fig. 6a that the theoretically predicted tendency is correct: the translocation exponent α grows with increasing force. Nevertheless, quantitatively the MD-values are systematically smaller than the theoretically expected ones: $\alpha \approx 1.33$ for the large force and $\alpha \approx 1.06$ for the small force. This behavior closely corresponds to the results found by the Langevin MD method [25–27].

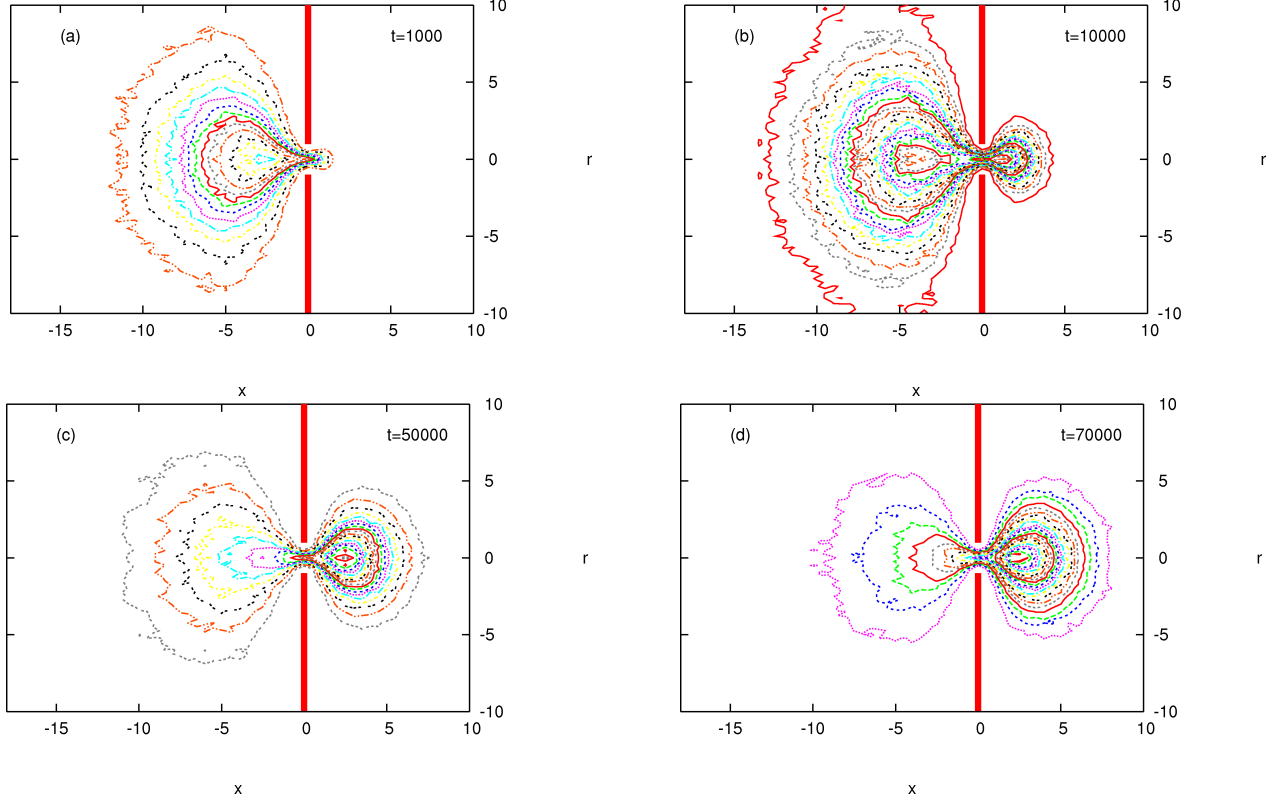


FIG. 4: (Color online) Contour plots of density corresponding to different time moments for the force $f = 2$ and the chain length $N = 100$. In (a) the density profile is plotted at $t = 1000$, (b) is for $t = 10^4$, (c) for $t = 5 \times 10^4$ and (d) for $t = 7 \times 10^4$.

Fig. 6b shows how the translocation time changes with force. For the long chains the exponent δ is very close to unity in a good agreement with the theoretical prediction. For a shorter chain $\delta \approx 1.37$ which is much smaller than the possible theoretical prediction within the trumpet scenario: $\delta \approx 1.7$.

2. Evolution of the translocation coordinate

Much information about the translocation process can further be obtained by examining the average value of the translocation coordinate $\langle s(t) \rangle$. The results for $\langle s(t) \rangle$ at different forces and chain lengths are shown in Fig. 7. It can be seen that for a fixed force the behavior is largely independent of the chain length, that is, the exponent β in $\langle s(t) \rangle \simeq t^\beta$ does not depend on N . Solely the plateau height which naturally (as for any Brownian motion on a finite interval) marks the long time limit $\langle s(t \rightarrow \infty) \rangle$ linearly depends on the chain length N .

One can also verify from Fig. 7 that the slope characterized by the exponent β becomes smaller with increasing strength of the driving force f . Namely, $\beta \approx 1.06$ for small forces and $\beta \approx 0.85$ for larger forces. These results could be compared with the corresponding theoretical predictions given by Eq. (2.34) and Eq. (2.30) (see also Fig. 2c). This basically reflects the same tendency which has already been seen in the $\langle \tau \rangle \propto N^\alpha$ scaling relationship. Apparently, the translocation time is defined as $\langle s(\langle \tau \rangle) \rangle = N$, i.e., $\langle \tau \rangle^\beta \sim N$ and we have $\beta \approx 1/\alpha$. This relationship holds well in our MD-simulation. Therefore, the fact that α grows with the force, which we have seen before, correlates with the decrease of the exponent β .

From Fig. 7 it also easily inferred that during the initial time period $\langle s(t) \rangle$ remains to a very good approximation almost constant. We identify this period with the blob initiation time (see Sec. II B), i.e., the time which is necessary to generate a first blob. In Fig. 7 this characteristic time τ_{init} manifests itself as a first crossover from a constant value

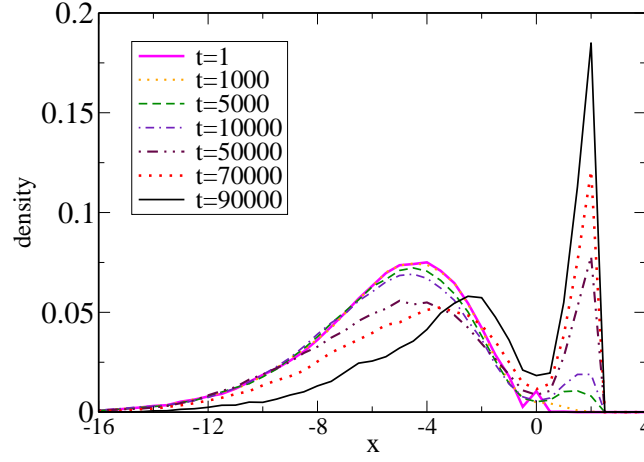


FIG. 5: (Color online) Density profiles (normalized to unity) as function of x -coordinate. In the time interval $0 < t \leq 70000$ the front moves toward the left, i.e., the moving domain grows at the expense of the rear part of the chain. At $t > 70000$ the second stage of the translocation, “suction in the pore”, sets in. On the trans-side (i.e. $x > 0$) the “crowding” effect can be seen.

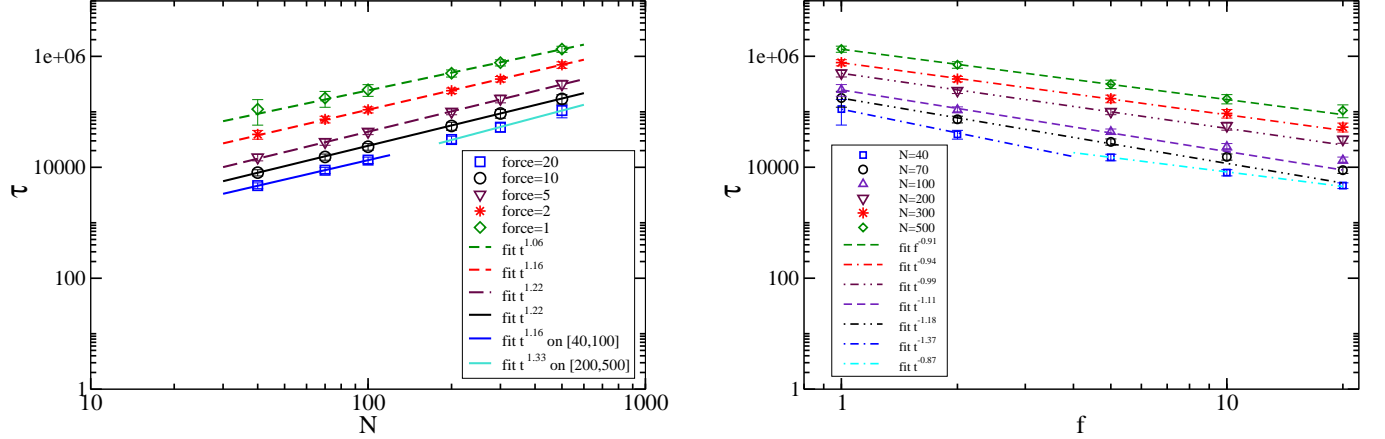


FIG. 6: (Color online) (a) The τ vs N for different forces f . The figure shows that $\tau \sim N^\alpha$, where α depends on the force. For small forces ($f = 1, 2$), the value of α is about 1.1, for larger forces ($f = 10, 20$), a crossover appears at $N^* = N \approx 100$. For chain lengths $N < N^*$ one has $\alpha \approx 1.16$ which is close to 2ν , whereas for $N > N^*$, $\alpha = 1.33$. (b) τ vs f for chain lengths $N = 40, 100, 200, 300, 500$. One finds $\tau \propto 1/f^\delta$ with $\delta \approx 1$. For short chains lengths the exponent δ is somewhat larger than 1.

(within 10%) to the scaling law $\langle s(t) \rangle \sim t^\beta$. The time τ_{init} is chain length independent but inversely proportional to the force f (cf. Eq. (2.2)). This conclusion is supported by Fig. 8 where the first crossover time τ_{init} is plotted against the force.

IV. CONCLUSIONS

In this work we derive scaling laws for the mean translocation time of a driven polymer chain through a narrow pore, based on the ideas of tensile force propagation along the polymer backbone [15, 16]. Our findings can be summarized as follows:

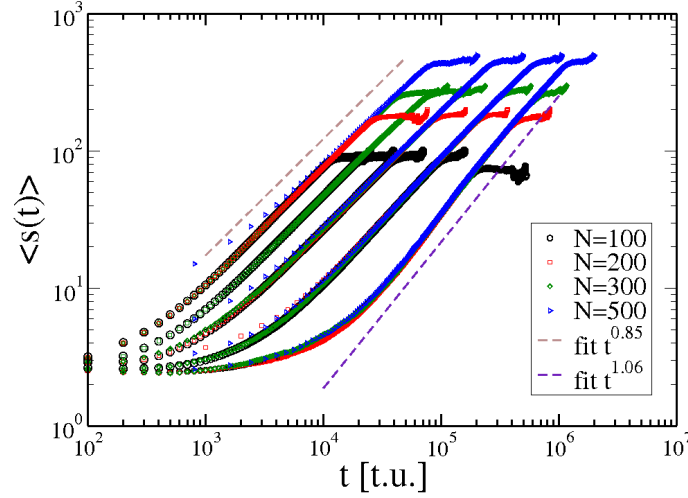


FIG. 7: (Color online) The average translocation coordinate $\langle s \rangle$ as function of time for 4 different chains lengths $N = 100, 200, 300, 500$ and 5 different forces $F = 1, 2, 5, 10, 20$. The force increases from right to left and the chain length increases from bottom to top. The translocation exponent β decreases for strong forces.

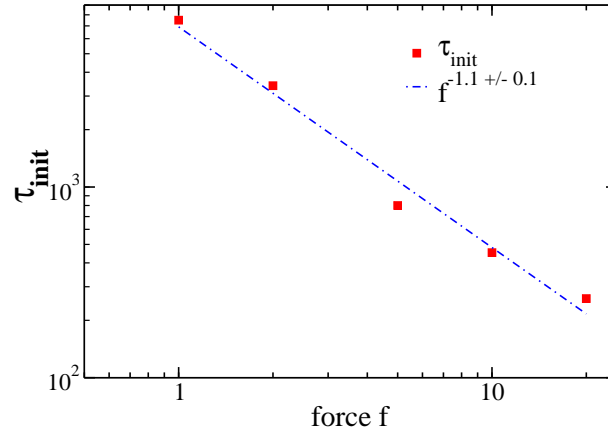


FIG. 8: (Color online) The time needed to create the first blob τ_{init} as a function of force for three different chains lengths. It is clear that this time is independent of the chain length and decreases approximately as $\tau_{\text{init}} \sim 1/f$. For large forces the force dependence appears to level off.

1. The translocation starts with the formation of initial Pincus blob (i.e., the first blob is generated immediately at the pore opening). The characteristic time of the blob initiation is given by Eq.(2.2). Our MD-simulation results essentially support the scaling prediction $\tau_{\text{init}} \sim 1/f$.
2. The initiation is followed by a tensile force transmission along the chain backbone which is governed by the local balance of driving and drag forces. For forces in the interval $N^\nu \ll af/k_B T < 1$ this leads to a trumpet regime (see Fig. 1). The corresponding translocation time is given by Eq. (2.26) where the first term, which corresponds to the force transmission characteristic time, prevails under the condition Eq. (2.27). As a result, depending on the force strength and on chain length (for Rouse dynamics), one expects a crossover from $N^{2\nu}/f^{1/\nu}$ to $N^{1+\nu}/f$, i.e., the translocation exponent α grows with increasing force f from $\alpha \approx 1.18$ to $\alpha \approx 1.59$.

One should note that the MD-simulation findings yield systematically smaller values for the translocation exponent: $\alpha \approx 1.06$ and $\alpha \approx 1.33$ for weak and strong forces respectively. This is in agreement with other simulation results [25–27] and differs from findings reported in ref. [28]. The mentioned slight overestimation of the translocation exponent α by the theory may be due to the role of fluctuations which are not accounted for within the quasi-static approximation used in this work. As for the force scaling, the theory predicts that the

scaling law ranges between $1/f^{1.66}$ and $1/f$ with the chain length increasing. Again the MD-simulation gives smaller exponents: $1/f^{1.37}$ and $1/f^{0.91}$ respectively.

3. Under the conditions, given by Eq. (2.27), the number of translocated segments $M(t)$ changes as $M(t) = c_0(\tilde{f}_a \tilde{t})^{1/(1+\nu)}$ (see Eq. (2.30)), i.e., in the scaling law $M(t) \sim (ft)^\beta$ the exponent $\beta \approx 0.63$ for relatively large forces. Our MD-simulation result gives a slightly larger value $\beta \approx 0.85$. The reason for that is the same as in the case of the scaling law $\langle \tau \rangle \sim N^\alpha$: recall that $\beta \approx 1/\alpha$.
4. For strong forces the tensile force transmission follows either the “stem-trumpet” ($1 \ll af/k_B T \ll N^\nu$) or the “stem” ($N^\nu \ll af/k_B T$) scenarios (see Fig. 1b, c). In both cases the translocation time can be estimated as $\langle \tau \rangle = C_1 \tau_0 N^{1+\nu}/\tilde{f}_a + C_2 \tau_0 N^{2\nu}/\tilde{f}_a$ where the first term dominates under condition $N^{1-\nu} \gg C_2/C_1$. In other words, the translocation scaling exponent grows from $\alpha = 2\nu$ to $\alpha = 1+\nu$ as the chain length N increases. This is in agreement with the results of LD-simulation [23] and also with the findings of Monte Carlo investigations[31].

We believe that the present approach leads to a consequent and physically plausible theory of driven translocation dynamics even though the theoretical predictions regarding scaling coefficients do not fully agree with data from computer experiments. The theory is based on the assumption that drag and driving forces equal one another during the process of chain threading through the pore. Since at the present level of theoretical treatment fluctuations are not taken into account, further developments of the theory should try to incorporate fluctuations too. Also the analytical model totally ignores additional resistance forces which are imposed by the pore and by the over-crowded beads at the pore exit (as it can be seen from Fig. 5). These forces should be included in the general force balance given by Eq. (2.5). On the other hand, these resistance forces make the translocation dynamics even more sluggish, so that one can not explain thus the observed decrease of the translocation exponents as compared to the theoretical prediction. In principle, one could extend the present consideration on the case of attractive pores where entering monomers may be captured and reside for a while in the pore. Such studies have been carried out recently [33, 34]. One should note, however, that this effect does not alter the scaling laws for translocation even though the some additional details of the process become thereby important. Evidently, more work is therefore needed until a full understanding and entirely satisfactory description of translocation dynamics is achieved.

V. ACKNOWLEDGMENTS

We should like to thank K.L. Sebastian and P. Rowghanian for fruitful discussions. A. Milchev thanks the Max-Planck Institute for Polymer Research in Mainz, Germany, for hospitality during his visit in the institute. A. Milchev and V. Rostiashvili acknowledge support from the Deutsche Forschungsgemeinschaft (DFG), grant No. SFB 625/B4.

Appendix A: Integral and differential forms of the material conservation law

Here we demonstrate why the calculation, performed in ref. [16], leads to a scaling result for τ_1 which deviates from the one given by Eq. (2.23) in Section II C. In contrast to the *integral form* of the material balance equation, given by Eq. (2.14) and used in the present work, in ref. [15, 16] one uses its *differential form* (cf. Eq. (5) in ref. [16]):

$$[\rho(x)\Sigma(x)]_{x=-X(t)} \left\{ \frac{dX(t)}{dt} + v(t) \right\} = \frac{dN(t)}{dt} \quad (\text{A1})$$

As before, $\rho(x) \simeq g(x)/\xi(x)^3$ is the local density and $\Sigma(x) \simeq \xi(x)^2$ stands for the cross-sectional area so that $\chi(x) = \rho(x)\Sigma(x)$ can be seen as the linear density.

One may readily see that the differential representation of the material conservation, Eq.(A1), suffers from the problem that the linear density $\chi(x)|_{x=-X(t)} = [\xi(x)/a]^{1/\nu-1}/a|_{x=-X(t)}$ does not exist because it diverges! Indeed, it is evident from Eq. (2.12) that $\xi(x)$ at $x = -X(t)$ has an integrable singularity. The physical reason for such behavior is clear: the force at the free boundary is zero, therefore, the tensile blob size goes to infinity (cf. Eq. (2.10)). Because of this, one should use from the very beginning the integral form Eq. (2.14) and may turn to the differential equation for $X(t)$ (cf. Eq. (2.20)) only after calculation of the involved integral.

Instead, Sakaue [15, 16] introduces a “cut-off” $x = -X(t) + \xi_X(t)$, where $\xi_X(t)$ is the “largest blob” given by Eq. (2.13). The implementation of the “largest blob” $\xi_X(t)$ as well as the relationships given by Eq. (2.11) (at $X(t) \gg k_B T/f$) and Eq. (2.15) in Eq.(A1) leads eventually to a differential equation for the front location $X(t)$ (in

dimensionless units):

$$\tau_0 \left[\tilde{X}(t)^{\omega+1} \tilde{f}_a^{\omega+2-z} - c_0 \tilde{X}(t) \tilde{f}_a^{2-z} \right] \frac{d\tilde{X}(t)}{dt} = 1 \quad (\text{A2})$$

where $\tilde{X}(t) = X(t)/a$, $\tilde{f}_a = af/k_B T$, $\omega = (1 - \nu)(z - 2)/\nu(z - 1)$, and c_0 is a numerical coefficient. The solution of this equation reads (cf. Eq. (2.22))

$$t = t_0 + \tau_0 \tilde{f}_a^{\omega+2-z} \tilde{X}(t)^{\omega+2} \left[1 - c_0 / \tilde{X}(t)^{\omega} \tilde{f}_a^{\omega} \right] \quad (\text{A3})$$

Finally, by equating $\tilde{X}(\tau_1) = N$, Sakaue obtains the characteristic time

$$\tau_1 \sim \tau_0 \tilde{f}_a^{\omega+2-z} N^{(\omega+2)\nu} \quad (\text{A4})$$

which differs from our result, given by Eq. (2.23). In the case of Rouse dynamics ($z = 2 + 1/\nu$), the scaling law Eq. (A4) leads to $\alpha = (1 + \nu + 2\nu^2)/(1 + \nu) \approx 1.43$ and $\delta = 1/(1 + \nu) \approx 1.26$. Despite the fact that this value for the α -exponent correlates better with our MD-findings, one may doubt if the calculation based on the “cut-off” trick is trustworthy. Actually, this “cut-off” trick makes the “trumpet” effectively shorter so that Sakaue’s characteristic time $\tau_1 \sim N^{1.43}/f^{1.26}$ is smaller than ours $\tau_1 \sim N^{1.59}/f$.

Contrary to Sakaue’s calculation, we use the *integral* form of the material conservation law Eq. (2.14) where the integral term can be calculated *exactly* (without resorting to any “cut-off” trick). By making use of the closure relation, Eq. (2.15), and the relationship for the translocated monomers, $M(t)$ Eq. (2.17), we derive a differential equation for $\tilde{X}(t)$, Eq. (2.20), which differs from the corresponding Eq. (A2).

-
- [1] M. Zwolak, M. Di Ventra, Rev. Mod. Phys. **80**, 141 (2008).
 - [2] D. Branton, *et al.*, Nat. Biotech. **26**, 1146 (2008).
 - [3] M. van der Laan, *et al.* Nat. Cell Biol. **9**, 1152 (2007).
 - [4] A. Aksimentiev, Nanoscale, **2**, 468 (2010).
 - [5] D. K. Lubensky, D.R. Nelson, Biophys. J. **77**, 1824 (1999).
 - [6] M. Muthukumar, J. Chem. Phys. **111**, 10371 (1999).
 - [7] S.-S. Chern, A.E. Cárdenas, R.D. Coalson, J. Chem. Phys. **115**, 7772 (2001).
 - [8] O. Flomenbom, J. Klafter, Phys. Rev. E, **68**, 041910 (2003).
 - [9] P. Rowghanian, A.Y. Grosberg, J.Phys.Chem. B **115**, 14127 (2011).
 - [10] J. L. A. Dubbeldam, V. G. Rostiashvili, A. Milchev, T. A. Vilgis, Europhys. Lett. **79**, 18002 (2007).
 - [11] H. Vocks, D. Panja, G. T. Barkema, R. C. Ball, J. Phys.: Cond. Mat. **20**, 095224 (2008).
 - [12] Y. Kantor, M. Kardar, Phys. Rev. E, **69**, 021806 (2004).
 - [13] A. Milchev, J. Phys.: Cond. Mat. **23**, 103101 (2011).
 - [14] J. L. A. Dubbeldam, V. G. Rostiashvili, A. Milchev, T. A. Vilgis, Phys. Rev. E **83**, 011802 (2011).
 - [15] T. Sakaue, Phys. Rev. E **76**, 021803 (2007).
 - [16] T. Sakaue, Phys. Rev. E **81**, 041808 (2010).
 - [17] M. Wanunu, W. Morrison, Y. Rabin, A.Y. Grosberg, A. Meller, Nat. Nanotechnol. **5**, 160 (2009).
 - [18] A.Y. Grosberg, Y. Rabin, J. Chem. Phys. **133**, 165102 (2010).
 - [19] S.W. Kowalczyk, A.Y. Grosberg, Y. Rabin, C. Dekker, Nanotechnology **22**, 315101 (2011).
 - [20] F. Brochard-Wyart, H. Hervet, P. Pincus, Europhys. Lett. **26**, 511 (1994).
 - [21] F. Brochard-Wyart, Europhys. Lett. **30**, 387 (1995).
 - [22] P.-G. de Gennes, *Scaling Concept in Polymer Physics*, Cornell University Press, Ithaca, 1979.
 - [23] K. Luo, S.T. T. Ollila, I. Huopaniemi, T. Ala-Nissila, P. Pomorski, M. Karttunen, S-C. Ying, A. Bhattacharya, Phys. Rev. E **78**, 050901(R), (2008).
 - [24] A. Bhattacharya, W.H. Morrison, K. Luo, T. Ala-Nissila, S.-C.Ying, A. Milchev, K. Binder, Eur. Phys. J. E **29**,423 (2009).
 - [25] V.V. Lehtola, R.P. Linna, K. Kaski, Phys. Rev. E **78**, 061803 (2008).
 - [26] V.V. Lehtola, R.P. Linna, K. Kaski, Europhys. Lett. **85**, 58006 (2009).
 - [27] V.V. Lehtola, R.P. Linna, K. Kaski, Phys. Rev. E **82**, 031908 (2010).
 - [28] K. Luo, T. Ala-Nissila, S-C. Ying, R. Metzler, Europhys. Lett. **88**, 68006 (2009).
 - [29] A.J. Storm, C. Storm, J. H. Chen, H. W. Zandbergen, J.-F. Joanny, C. Dekker, Nano Lett. **5**,1193 (2005).
 - [30] A.J. Storm, J. H. Chen, H. W. Zandbergen, C. Dekker, Phys. Rev. E **71**, 051903 (2005).
 - [31] M.G. Gauthier, G.W. Slater, J. Chem. Phys. **128**, 205103 (2008).
 - [32] A. Bhattacharya, K. Binder, Phys. Rev. E **81**, 041804 (2010).
 - [33] K. Luo, T. Ala-Nissila, S-C. Ying, A. Bhattacharya, Phys. Rev. Lett. **99**, 148102 (2007).
 - [34] K. Luo, T. Ala-Nissila, S-C. Ying, A. Bhattacharya, Phys. Rev. E **78**, 061918 (2008).